doi:10.1111/evo.12407

LEVERS AND LINKAGES: MECHANICAL TRADE-OFFS IN A POWER-AMPLIFIED SYSTEM

Philip S. L. Anderson,[1,2] Thomas Claverie,[3,4] and S. N. Patek[1]

[1]*Department of Biology, Duke University, Durham, North Carolina 27708*

[2]*E-mail: philip.anderson@duke.edu*

[3]*Laboratoire ECOSYM, UMR 5119, Université de Montpellier 2, Place Eugène Bataillon cc93, 34095 Montpellier, France*

[4]*CUFR de Mayotte, Route nationale 3, 97660 Dembeni, France*

Received September 11, 2013
Accepted March 7, 2014

Mechanical redundancy within a biomechanical system (e.g., many-to-one mapping) allows morphologically divergent organisms to maintain equivalent mechanical outputs. However, most organisms depend on the integration of more than one biomechanical system. Here, we test whether coupled mechanical systems follow a pattern of amplification (mechanical changes are congruent and evolve toward the same functional extreme) or independence (mechanisms evolve independently). We examined the correlated evolution and evolutionary pathways of the coupled four-bar linkage and lever systems in mantis shrimp (Stomatopoda) ultrafast raptorial appendages. We examined models of character evolution in the framework of two divergent groups of stomatopods—"smashers" (hammer-shaped appendages) and "spearers" (bladed appendages). Smashers tended to evolve toward force amplification, whereas spearers evolved toward displacement amplification. These findings show that coupled biomechanical systems can evolve synergistically, thereby resulting in functional amplification rather than mechanical redundancy.

KEY WORDS: **Biomechanics, kinematic transmission, mantis shrimp, phylogenetic comparative methods, trade-offs.**

The manipulation of a simple mechanical system to generate a wide array of functions is a foundation of evolutionary diversification. A pattern of diversification can be driven by the underlying geometry and morphology of the mechanical system. For example, the evolution of wings led to the diversification of bird wings into a broad range of flight-based lifestyles within the physical constraints of airfoil function (Rayner 1988). Similarly, the advent of the vertebrate lower jaw led to a massive diversification in early vertebrates into a range of feeding behaviors based on exploiting simple lever mechanics (Anderson et al. 2011).

One mode of evolutionary diversification occurs through mechanical redundancy, such that more than one configuration yields the same output (many-to-one mapping; Alfaro et al. 2005). Many-to-one mapping posits that mechanical systems with more than one degree of freedom will have multiple morphological solutions for the same emergent function (Alfaro et al. 2004, 2005; Wainwright et al. 2005). One example is the four-bar linkage system, in which different morphologies can produce identical mechanical outputs, allowing for morphological variation in the linkage without altering its basic function (Alfaro et al. 2004). Many-to-one mapping in the teleost four-bar linkage system likely promoted diversification, given that the most common biomechanical output among teleost four-bar systems is the one with the most morphological solutions (Alfaro et al. 2005). In other words, the more morphological solutions available for a given biomechanical output, the more opportunity there is for morphological diversification without compromising the mechanics.

Many-to-one mapping is generally identified at the level of a single mechanism with a single mechanical output such as the linkage system of teleost jaws. However, biological structures are typically interconnected and mechanically coupled to each other. For example, the teleost linkage system opens the jaws and buccal cavity while also aided by a lever system that actuates buccal expansion for suction feeding (Collar and Wainwright 2006). The same principle of many-to-one mapping should hold for these coupled mechanical systems given that each mechanism produces independent mechanical outputs. It should be possible for evolutionary changes in one mechanism to be counterbalanced

© 2014 The Author(s).

EVOLUTION
INTERNATIONAL JOURNAL OF ORGANIC EVOLUTION

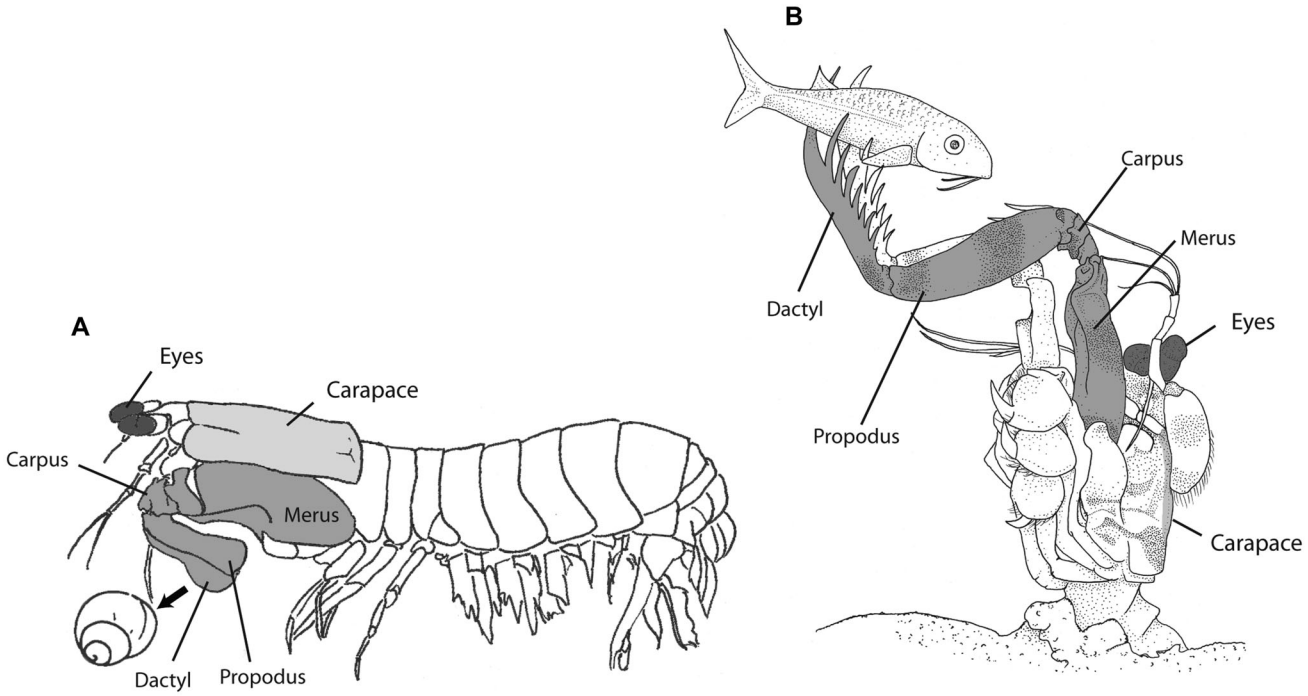

Figure 1. Variation of the stomatopod raptorial appendage is associated with several types of prey capture behaviors, two of which are smashing and spearing. (A) The smasher, *Gonodactylus smithii*, strikes hard-shelled prey with hammer-shaped appendages. Sketch adapted from Cox et al. (2014). (B) The spearer, *Lysiosquillina maculata*, strikes free-swimming prey from its burrow using a long bladed appendage. Sketch adapted from de Vries et al. (2012).

by shifts in another to maintain a stable functional output during morphological diversification much like in single mechanisms (Alfaro et al. 2004, 2005). However, it is also possible that coupled systems may work to amplify mechanical effects instead of balancing them.

Here, we examine the evolutionary dynamics of a coupled mechanical system in mantis shrimp (Stomatopoda). Stomatopods (mantis shrimp) wield an ultrafast power-amplified raptorial strike system (Patek et al. 2004; Fig. 1). Several stomatopod clades (spearers) use their raptorial appendages to spear evasive prey from an ambush position using long, thin appendages, often with several spines along the edge (Caldwell and Dingle 1976; deVries et al. 2012). One derived clade (the Gonodactyloidea: "smashers") uses this same appendage like a hammer to smash hard-shelled prey (Caldwell and Dingle 1976; Patek et al. 2004). Smashers achieve incredibly high peak strike speed (up to 30.6 m/s), acceleration (up to 154 km/s^2), and impact forces (1500 N) (Patek et al. 2004; Patek and Caldwell 2005; Cox et al. 2014). Spearers, on the other hand, strike more slowly than smashers, with peak speed of 6 m/s and acceleration up to 12.5 km/s^2 (deVries et al. 2012). The basal stomatopod group (*Hemisquillidae*) uses an intermediate appendage form, lacking hammer or spines, to dislodge and break hard-shelled prey.

The stomatopod raptorial strike system comprises a coupled lever and four-bar linkage mechanism (Patek et al. 2004, 2007; deVries et al. 2012; Fig. 2). A power-amplifying spring mechanism stores energy that, when released, creates a faster strike than would be possible from muscle action alone (Patek at al. 2004). This power amplification system drives a four-bar linkage mechanism that transfers force and movement into a swinging appendage that acts as a lever (Patek et al. 2007; McHenry et al. 2012; Fig. 2).

Levers and four-bar linkages are both mechanisms that work to transmit force and movement. A lever is a single beam that is rotated around a fulcrum by an input force (Fig. 2). This input force is transferred to the output at a percent efficiency based on the configuration of the lever. The percent of input force transferred to the output is called mechanical advantage (MA). There is a negative relationship between force efficiency and displacement in a lever. A lever that transmits a high level of force does so at the expense of displacement (Fig. 2). In contrast to lever systems, linkages transfer force and displacement through a series of rigid beams connected to each other at rotation points (Suh and Radcliffe 1978; Fig. 2). Kinematic transmission (KT) in linkages is defined as the ratio of the rotation of the output bar to rotation of the input bar (Anker 1974; Barel et al. 1977). As KT increases,

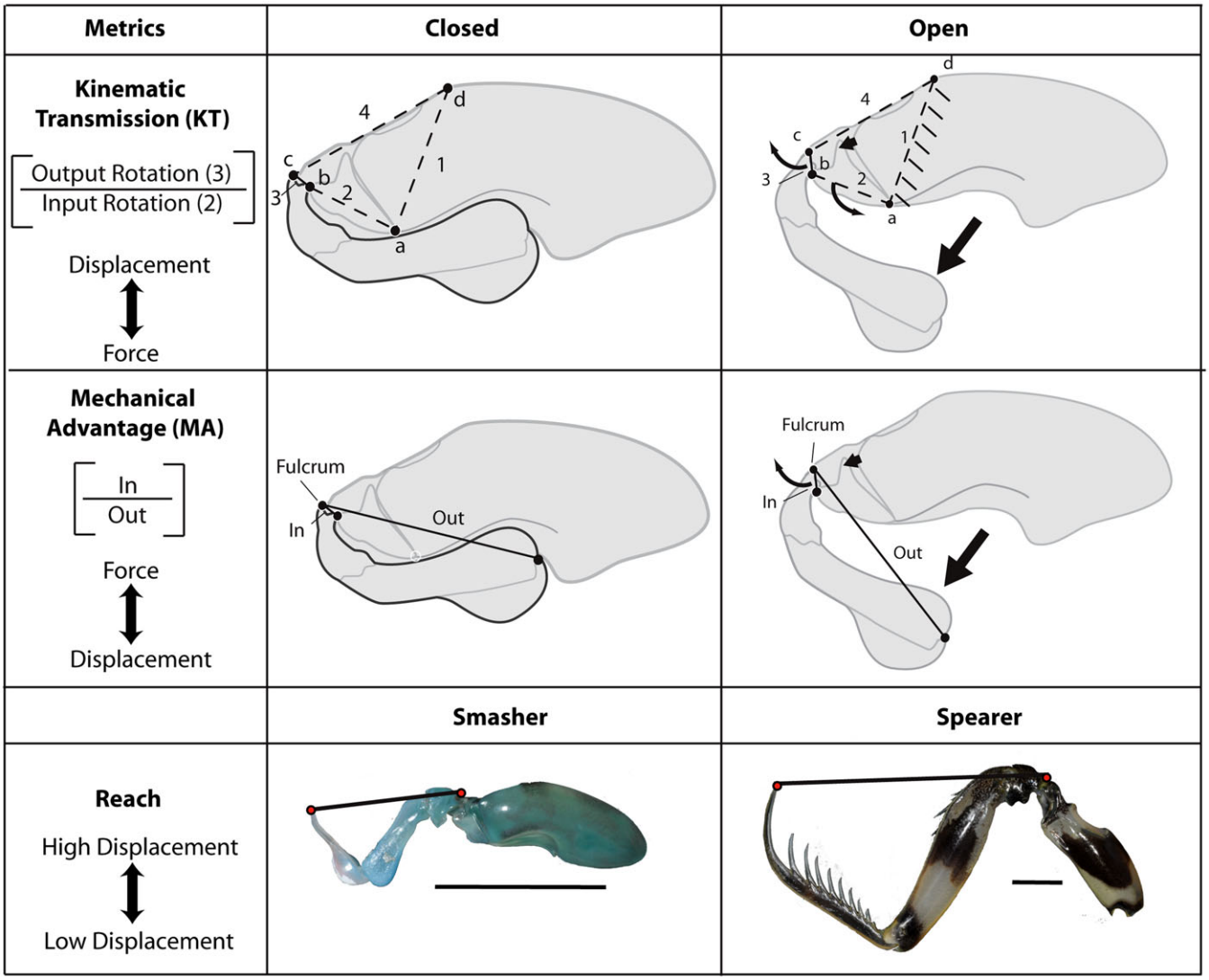

Figure 2. A series of biomechanical metrics is used to explore the evolution of the stomatopod raptorial appendage. These include kinematic transmission (KT), mechanical advantage (MA), and Reach. KT is the displacement or movement transferred through a four-bar linkage. The linkage mechanism consists of four links (link 1: merus; link 2: meral-V; link 3: carpus; link 4: muscle spanning the carpus and merus) and four pivots (a–d). When unloading during a strike, the meral-V (link 2) rotates distally around pivot *a* and pushes pivot *b* distally with it. Consequently, link 3 rotates the propodus and dactyl to strike. KT is measured as link 3 (output) rotation divided by link 2 (input) rotation. MA represents the force transfer efficiency of a lever system that transmits the movement from the linkage system to the end of the propodus. The lever system is a third-order lever in which the point of rotation (the "fulcrum") is at the proximal end of the carpus, the in-lever is the distance from the fulcrum to where the meral-V contacts the carpus during rotation, and the out-lever is the distance from the fulcrum to the end of the propodus. During a strike, the meral-V pushes against the carpus, the carpus rotates around the fulcrum (pivot *c* of the linkage), and the propodus rotates distally. The MA of the lever system is the ratio of the in-lever (In) and out-lever (Out). Reach represents the position of the appendage when the dactyl extends to stab the target. Reach extends from the proximal end of the carpus to the tip of the dactyl while the dactyl is held at 90° to the propodus. All appendages are oriented distal to left and dorsal to top of the page. Sketches adapted from McHenry et al. 2012. The photos depict the smasher, *Gonodactylus smithii*, and spearer, *Lysiosquillina maculata*. The photos have been altered digitally to position the dactyl at 90° relative to the propodus. Scale bars = 15 mm.

more output rotation occurs relative to the input rotation; therefore, the linkage transmits more displacement. Inversely, a lower KT results in less displacement, but yields greater force transmission (Fig. 2). Thus, force and displacement are inversely related in a linkage system (Barel et al. 1977; Westneat 1994), just as they are in a lever system.

Both the lever system and linkage system are defined by a force–displacement trade-off. This means that the mechanical

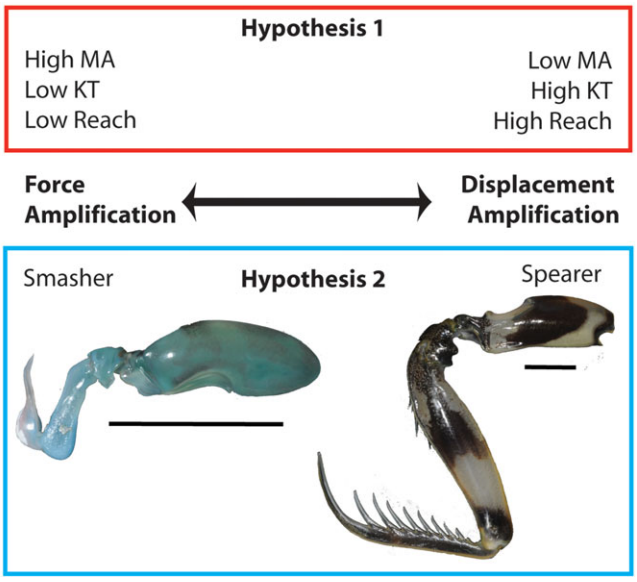

Figure 3. We tested two hypotheses in this study. The first hypothesis states that the three biomechanical metrics exhibit correlated evolution. In particular, we predict that the stomatopod appendage system shows either amplification of force or displacement. Correlated evolution of displacement amplification (right side of figure) occurs if high kinematic transmission (KT) and Reach are correlated with each other and with low mechanical advantage (MA). Correlated evolution of force amplification (left side of figure) occurs if low KT and Reach are correlated with each other and high MA. The second hypothesis is supported if the two major appendage types show divergent evolution toward force or displacement amplification. We predict that smashers evolve toward force amplification (high MA, low KT, and low Reach) and spearers + *Hemisquilla* evolve toward displacement amplification (low MA, high KT, and high Reach). The photos depict the smasher, *Gonodactylus smithii*, and spearer, *Lysiosquillina maculata*. Scale bars = 15 mm.

outputs of the two mechanisms can amplify each other (by both maximizing force or displacement) or balance each other in a manner similar to many-to-one mapping (the linkage could maximize force whereas the lever maximizes displacement leaving the resulting overall mechanical output stable).

Where the mantis shrimp appear on this force–displacement spectrum likely depends on their feeding strategies. Smashers require substantial force to break open hard-shelled prey, suggesting a strike system focused on force amplification (high MA and low KT). However, smashers are also considerably faster than spearers; this is counterintuitive, given that studies of fish four-bar systems typically associate fast movement with displacement amplification (high KT values; Westneat 1994). A recent mathematical model of the mantis shrimp four-bar system showed that increasing the KT of the linkage might actually reduce overall strike speed when the effects of drag force are included (McHenry et al. 2012); a higher KT yielded greater displacement and greater drag forces acting against the appendage. Spearers likely require displacement amplification (high KT and low MA) as they typically ambush prey from their burrows. Increasing displacement during a strike increases the volume of water from which prey can be ambushed. These factors imply that the raptorial appendage system in stomatopods is governed by the basic force/displacement trade-off inherent to levers and linkages.

We tested the relationship between force and displacement in the coupled four-bar and lever systems of the stomatopod raptorial appendage and examined how this relationship is associated with the evolutionary diversification of the appendage into smashers and spearers. We measured three biomechanical metrics associated with force and displacement in the stomatopod appendage: KT of the four-bar linkage system, MA of the lever arm, and Reach of the appendage (the extension of the appendage from the rest of the body; Fig. 2). We tested two hypotheses regarding the mechanical evolution of the stomatopod raptorial appendage (Fig. 3).

The first hypothesis states that biomechanical changes in the four-bar linkage system are amplified by congruent changes in the lever and appendage Reach. For example, congruent displacement amplification would consist of an increase in linkage KT, a decrease in lever MA, and an increase in Reach: all of the changes increase the overall displacement and therefore show congruent amplification. Support for this hypothesis would indicate that coupled mechanical systems can be both morphologically independent and functionally coupled, thereby enabling amplification of mechanical outputs (Claverie et al. 2011; Claverie and Patek 2013). An alternative hypothesis is that the lever and linkage mechanisms exhibit independent evolution, resulting in various combinations of mechanical outputs (e.g., a counterbalancing increase in KT coupled with an increase in MA). This is analogous to the many-to-one mapping pattern, in which mechanical outputs occur via multiple combinations of components, thereby allowing the components to evolve independently. We predict that stomatopods will show evidence of correlated changes in the raptorial appendage across phylogeny and that these changes will yield amplified mechanical effects. Specifically, KT, MA, and Reach will be correlated across phylogeny, and stomatopods will either amplify displacement (high KT, low MA, and high Reach) or force (low KT and high MA). Reach represents variation in displacement and is unrelated to force amplification (Fig. 2).

The second hypothesis states that directed evolutionary changes in the mechanical systems occurred during the diversification of mantis shrimp, such that smashers evolved toward force amplification and spearers toward displacement amplification. By comparing models of trait evolution for KT, MA, and

Table 1. Stomatopod taxa used in this study including the museum where the specimens were measured.

Family	Genus	Species	Museum
Gonodactyloidea			
Gonodactylidae	*Gonodactylaceus*	*falcatus*	NMNH
Gonodactylidae	*Gonodactylellus*	*espinosus*	NMNH
Gonodactylidae	*Gonodactylus*	*childi*	NMNH
Gonodactylidae	*Gonodactylus*	*chiragra*	NMNH
Gonodactylidae	*Gonodactylus*	*platysoma*	NMNH
Gonodactylidae	*Gonodactylus*	*smithii*	NMNH
Gonodactylidae	*Neogonodactylus*	*bahiahondensis*	NMNH
Gonodactylidae	*Neogonodactylus*	*bredini*	NMNH
Gonodactylidae	*Neogonodactylus*	*oerstedii*	NMNH
Odontodactyloidae	*Odontodactylus*	*havanensis*	NMNH
Odontodactyloidae	*Odontodactylus*	*latirostris*	NMNH
Odontodactyloidae	*Odontodactylus*	*scyllarus*	NMNH
Protosquillidae	*Chorisquilla*	*excavata*	NMNH
Protosquillidae	*Chorisquilla*	*tweediei*	NMNH
Protosquillidae	*Enchinosquilla*	*guerinii*	NMNH
Protosquillidae	*Haptosquilla*	*glyptocercus*	NMNH
Protosquillidae	*Haptosquilla*	*trispinosa*	NMNH
Takuidae	*Taku*	*spinocarinatus*	AM
Hemisquilloidea			
Hemisquillidae	*Hemisquilla*	*australiensis*	AM
Hemisquillidae	*Hemisquilla*	*californiensis*	NMNH
Lysiosquilloidea			
Lysiosquillidae	*Lysiosquillina*	*maculata*	NMNH
Lysiosquillidae	*Lysiosquillina*	*sulcata*	AM
Nannosquillidae	*Alachosquilla*	*vicina*	NMNH
Nannosquillidae	*Austrosquilla*	*tsangi*	AM
Tetrasquillidae	*Heterosquilla*	*tricarinata*	AM
Parasquilloidea			
Parasquillidae	*Pseudosquillopsis*	*marmorata*	NMNH
Pseudosquilloidea			
Pseudosquillidae	*Pseudosquilla*	*ciliata*	NMNH
Pseudosquillidae	*Pseudosquillana*	*richeri*	NMNH
Pseudosquillidae	*Raoulserenea*	*hieroglyphica*	NMNH
Pseudosquillidae	*Raoulserenea*	*ornata*	NMNH
Pseudosquillidae	*Raoulserenea*	*oxyrhyncha*	NMNH
Squilloidea			
Squillidae	*Busquilla*	*plantei*	NMNH
Squillidae	*Fallosquilla*	*fallax*	AM
Squillidae	*Harpiosquilla*	*harpax*	NMNH
Squillidae	*Kempina*	*Mikado*	AM
Squillidae	*Squilla*	*Empusa*	NMNH

Museum Key: AM = Australian Museum, Sydney; NMNH = National Museum of Natural History at the Smithsonian Institute, Washington, DC. Smasher taxa are highlighted in gray.

Reach across the stomatopod tree, we tested whether the three metrics show a random walk pattern of evolution, or a more directed evolutionary pattern based on one or more optimal values. We predict that models of trait evolution will show directed evolution for KT, MA, and Reach, with smashers and spearers evolving toward separate hypothetical optima.

Methods

MATERIALS

Our dataset consists of 36 species from six superfamilies of Stomatopoda (Table 1). The majority of these taxa can be assigned to one of the two appendage types: smashers (18 taxa) and spearers (16 taxa). The final two taxa, *Hemisquilla australiensis* and

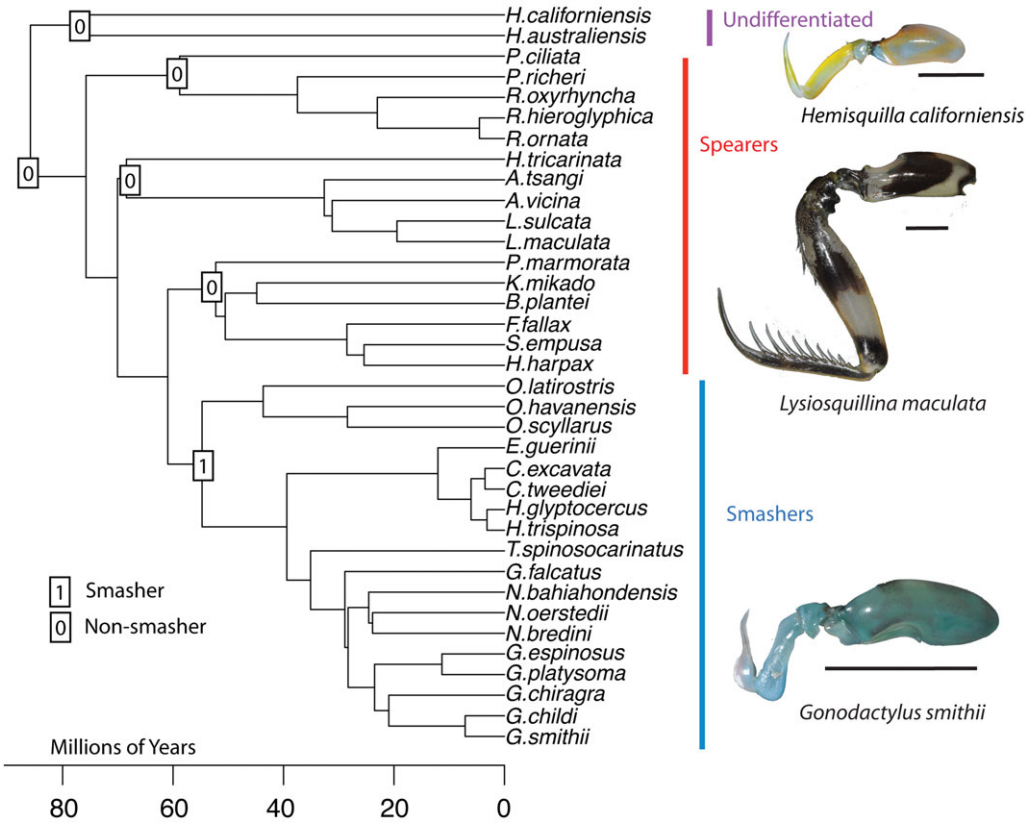

Figure 4. Using a previously published phylogeny that included a subset of stomatopod taxa (Porter et al. 2010), our analysis included 36 taxa from 11 families and six superfamilies as shown here. Undifferentiated taxa, such as the two *Hemisquilla* species, are found at the base of the tree, whereas smashers are a clade nested within the spearers. Ancestral reconstructions of appendage type are labeled at the basal nodes as either "smasher" (1) or "nonsmasher" (0). All nodes tipwards of an ancestor label share that appendage type. Appendages are oriented distal to left and dorsal to top of the page. Scale bars = 15 mm. Tree modified from Claverie and Patek 2013.

H. californiensis, do not fit into either appendage category, but are of interest as *Hemisquilla* is the basal-most stomatopod genus (Ahyong and Jarman 2009; Porter et al. 2010). Throughout this study, we group these two taxa with the spearers, given that the smashers represent a single, derived clade within the phylogeny (Fig. 4). The specimens are currently housed at the Smithsonian Museum of Natural History and Patek Laboratory. Specimens were photographed with the raptorial appendage in lateral view using a digital camera (12 megapixel, Nikon D300; AF Micro-NIKKOR 60 mm F/2.8D or 105 mm F/2.8D macro lenses, Nikon Inc., Melville, NY; and EM-140 DG macro-flash, Sigma Corp., Ronkonkoma, NY). Photographs were used to measure the kinematic and morphological traits as described below.

MECHANICAL TRAITS

Kinematic transmission

Mantis shrimp transmit force from an elastic mechanism in the merus segment to the rapidly rotating dactyl and propodus segments via a four-bar linkage system (Fig. 2; Patek et al. 2004, 2007; McHenry et al. 2012). Briefly, we describe the four links that comprise this system. Link 1 is a fixed link located along the proximal merus exoskeleton. Link 2 is the input link located along the meral-V. The carpus forms link 3, the coupler link. Link 4 is the follower link formed by the contracted extensor muscle that runs between the carpus and merus. These four links are connected by four pivots (Fig. 2).

A coordinated sequence of link rotations loads and releases the strike. Link 2 is rotated proximally by muscles during strike preparation to compress the spring mechanism. Link 2 is held in place by a latch mechanism in the merus. When link 2 is released, it rotates distally around pivot *a* (the ventral articulation of the meral-V) and pushes link 3 forward and outward through the connection of links 2 and 3 at pivot *b* (the lateral articulation between the meral-V and carpus). Link 3's rotation around pivot *c* causes the outward swing of the propodus that is also connected to pivot *c* through the articulation of the carpus to the propodus.

KT is the ratio of output rotation and input rotation. In this case, the input rotation is performed by link 2 (the meral-V). This

movement is transmitted to link 3 (the carpus). The ratio of meral-V rotation to carpus rotation is KT (Fig. 2). A high KT indicates that a small input rotation yields a high output rotation.

We measured KT across all 36 taxa using a simulation of the link rotation during a strike (R version 3.0.1, R Development Core Team 2012). Link 2 (input) rotation is well defined in stomatopods: the meral-V rests in the open, maximal rotation position, and can be compressed to the starting position by folding the meral-V against the merus. These start and end positions are biologically relevant as they represent the start and end position of the spring mechanism used during the animals natural strike behavior. Using these start and end positions, we mathematically simulated the rotation of the appendage and measured KT. Although KT is usually measured statically (Westneat 1994; Anderson and Westneat 2009), it is actually dynamic; the KT changes constantly during rotation as the orientation of the four bars shifts (Patek et al. 2007). To account for this, we sampled KT at regular intervals (0.1°) throughout the strike motion and selected the minimum KT. Measuring static KT usually involves picking a set input angle and measuring the resulting output angle (see Alfaro et al. 2004). This is a reasonable way to approximate KT for comparative analyses; however, as the various stomatopod species all have different degrees of input rotation (defined by the size and shape of the meral-V), we would be unable to standardize the KT across species if we used a single input value. Thus, we had to decide upon an arbitrary yet comparable measure of KT across all taxa and selected the minimum KT as it represents a conservative calculation.

Mechanical advantage

In a lever system, MA represents how much input force is translated into output force. Linkages can also be characterized in terms of MA (Uicker et al. 2003) and MA is often inversely correlated with static KT. To independently assess the linkage and lever systems, we defined MA in terms of the appendage lever system (although the lever and linkage share one common beam, their mechanical outputs are independent). MA is defined as the length of the propodus-carpus element rotating around pivot *c* of the linkage (where the carpus is attached to the merus via the extensor muscle). We define the in-lever as link 3 (distance between pivots *b* and *c*) of the four-bar system (Fig. 2). The out-lever is the distance between pivot *c* of the linkage and the tip of the propodus (Fig. 2). This makes a third-order lever system (Archimedes, 3rd century B.C.): the in-lever rotates around pivot *c* of the linkage and the out-lever is the swinging arm of the propodus.

Reach

We define Reach as the distance that the distal two segments of the appendage (propodus and dactyl) extend beyond the body during prey capture/acquisition. Reach therefore acts as a proxy for the range of potential prey capture during a strike without moving the body. A large Reach represents a greater potential strike range.

We used a measure of Reach based on a similar metric defined previously (Dingle and Caldwell 1978). Dingle and Caldwell measured the distance from the posterior edge of the merus to the tip of the dactyl when the appendage was oriented with predefined angles (130° between the merus and propodus, and 90° between the propodus and dactyl). The Reach metric used in this study is the distance from the proximal end of the propodus/carpus to the tip of the dactyl when the angle between the propodus and dactyl is 90° (Fig. 2). This length is the hypotenuse of a right triangle with sides defined as the propodus length (distance from the carpus/merus joint to the propodus/dactyl joint) and dactyl length (defined as the distance from the propodus/dactyl joint to the tip of the dactyl) and can be calculated using the Pythagorean theorem. Reach does not include merus length in its calculation. Our Reach is a more relevant measure for this study than the measure used by Dingle and Caldwell, because the merus is not part of the strike movement driven by the linkage. Reach as defined in our study will be highly correlated with overall body size. We account for this in our statistical analysis by including body size (measured as carapace length) as another predictor variable (see below).

All measurements (KT, MA, and Reach, as well as carapace length) were tested for normality using the Shapiro–Wilk test in R (R version 3.0.1, R Development Core Team 2012) and those with nonnormal distributions were log-transformed prior to performing the comparative analyses to bring their distributions closer to normal.

COMPARATIVE METHODS

Tree selection

The Stomatopoda consists of over 450 species and we performed these measurements on a representative subset of the total group. We used a pruned (from 49 taxa down to 36), time-calibrated version of a previously reported, molecular phylogenetic tree (Porter et al. 2010; time calibration from Claverie and Patek 2013; pruning done using ape version 2.73, R, Paradise et al. 2004). This tree (Fig. 4) is based on nucleotide sequence data from two nuclear (18S and 28S rDNA) and two mitochondrial (16S and cytochrome oxidase I) genes. The branch lengths are proportional to time based on a relaxed clock model of mutation rate (Ho and Phillips 2009) with hard-bound calibration points based on fossil occurrences (Claverie and Patek 2013). More details of the time calibration methods can be found in Claverie and Patek (2013).

Test of Hypothesis 1: phylogenetic generalized least square regression (PGLS)

To test Hypothesis 1 (Fig. 3: KT, MA, and Reach are correlated across stomatopod phylogeny), we used PGLS, (caper version

Table 2. Of the three biomechanical traits analyzed, only Reach is correlated with size.

y-Variable	Intercept	Coefficient	Std Error	*t*-Value	*P*-value	R^2	λ	Log-likelihood
KT (df = 2,34)	1.90*	0.012	0.034	0.341	0.735	0.0034	0.869	17.43
MA (df = 2,34)	−3.49*	0.053	0.055	0.967	0.34	0.027	1.00	−4.66
Reach (df = 2,34)	**−0.01**	**1.1**	**0.036**	**30.14**	**<0.001**	**0.964**	**0.902**	**14.61**

Mean values for each species were analyzed using PGLS. All continuous variables are log-transformed. The *x*-variable for all comparisons is carapace length. Statistically significant values are indicated in bold. The statistical results apply to the coefficient. An asterisk indicates that the intercept is significantly different than zero.

0.5, R, Orme et al. 2012). Delta (change in rates of evolution) and kappa (gradual vs. punctuated evolution) were fixed at 1 (assuming Brownian motion in both cases) whereas λ (phylogenetic signal) was estimated using a maximum likelihood method. Estimating λ this way allowed the model to deviate from a strict Brownian motion model of trait evolution. We also used PGLS to test the effects of potentially confounding variables (appendage type) on the relationship between kinematics and Reach. When PGLS is used with a categorical predictor alone (such as appendage type), it acts as a phylogenetically controlled *t*-test (Organ et al. 2007).

Because Reach is a linear measure, it will likely be strongly associated with body size. We tested this using PGLS to measure the relationship between Reach and carapace length (a proxy for body size). We also tested KT and MA against carapace length and compared models of association between the three metrics with and without size included as a predictor variable.

Test of Hypothesis 2: models of character evolution

We tested Hypothesis 2 (Fig. 3: Reach, KT, and MA evolve toward different optimal values in smasher and spearer clades) by applying maximum likelihood to test alternative adaptive models for our mechanical traits. We compared three models using the functions in OUCH, which estimate the Brownian motion rate parameter (σ^2), strength of selection (α), optimal trait values (θ), and support (Akaike information criterion corrected for finite sample sizes [AICc]) for each model. The first model is the basic Brownian motion model ($\alpha = 0$ and $\theta = 0$). The second model is a single-peak Ornstein Uhlenbeck (OU) model, which is a Brownian motion model pulled toward a single adaptive peak (θ) for each parameter (OUCH version 2.8–1, R [King and Butler 2009]). The third model is an OU model pulled toward two adaptive peaks, one for each appendage type (Butler and King 2004). This third model represents a situation in which smashing and spearing place different selective pressures on the linkage systems. As mentioned above, the two *Hemisquilla* taxa are included in the nonsmashers even though they do not conform to either appendage type. To test the effects of including *Hemisquilla*, model comparisons were also performed on a dataset in which these taxa were removed.

To test the multipeak model, it is necessary to assign an appendage type to the internal nodes of the tree. We estimate these node assignments using a likelihood method for ancestral state reconstruction based on a rerooting method (Yang et al. 1995) as implemented in phytools (phytools version 2.9, R, Revell 2012). Ancestral state reconstructions add a level of uncertainty to our analyses, as the specific reconstruction may have an effect on our results. However, smashers represent a monophyletic clade nested within the spearers + *Hemisquilla*, making the reconstruction straightforward (Fig. 4). All three models were run for KT, MA, and Reach. To explore the evolution of these characters visually, we also plotted a phylomorphospace using KT and Reach as the two axes (phytools version 2.9, Revell 2012).

Model selection was based on AICc (Burnham and Anderson 2002). Recent simulation work has called into question the use of AIC as a criterion for model selection in phylogenetic comparative methods and an alternative method has been proposed based on Monte Carlo methods using the R package pmc (Boettiger et al. 2012). This method estimates the power of statistical analyses, something rarely performed in comparative analyses. Given our relatively small tree (37 taxa), we tested the statistical power of our data using these methods and report the results in the Supporting Information.

Results

As expected, KT and MA show no significant association with carapace length (Table 2). Reach does show a significant association with carapace length (slope near to 1 and an intercept of 0) illustrating an almost isometric relationship between the two measures (Table 2). For subsequent analyses involving Reach, carapace length is included as a predictor to tease apart the associations between Reach and the other metrics.

HYPOTHESIS 1: TRAIT CORRELATIONS

In support of our predictions for Hypothesis 1, we found that KT and Reach show a significant positive association across stomatopod phylogeny (Fig. 5A, C, Table 3). Again, supporting our predictions, Reach and MA show a significant negative

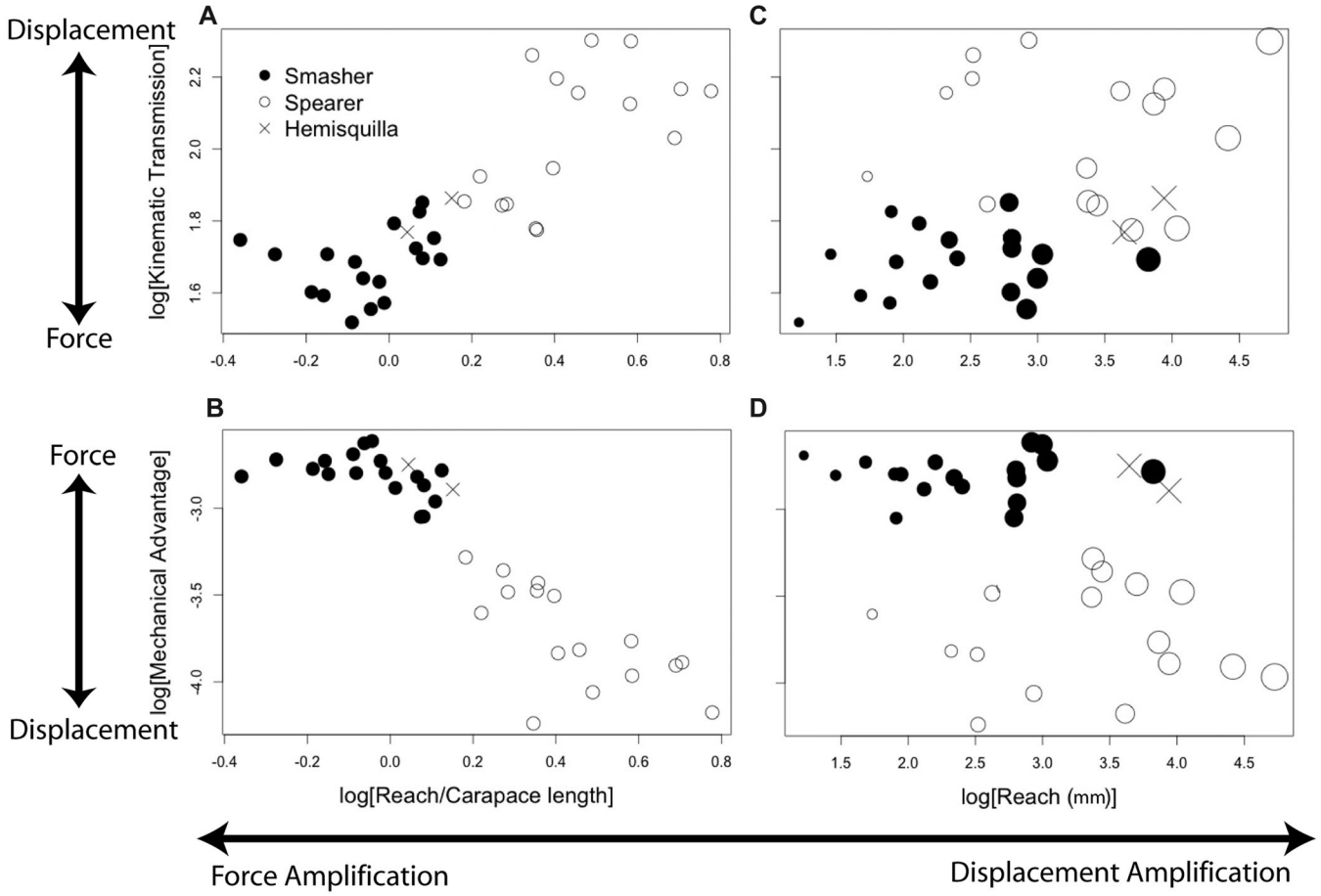

Figure 5. **The associations between Reach, mechanical advantage (MA), and kinematic transmission (KT) follow distinct associations and ranges across smashers (closed circles) and spearers (open circles). In (A) and (B), Reach has been divided by carapace length to account for variation in body size. In (C) and (D), Reach (not size corrected) is plotted with the size of each point proportional to carapace length. In the actual statistical analyses, we incorporated size using phylogenetic regression methods rather than simply dividing by size (see Methods). (A) As Reach/size increases, KT also increases, within and across mantis shrimp groups. The two *Hemisquilla* species (crosses) fall at the intersection of smashers and spearers. (B) The opposite trend occurs for MA: as Reach/size increases, MA decreases within and across mantis shrimp groups. (C) Reach that has not been divided by carapace size shows a more complex pattern. There is no linear correlation between KT and Reach either across or among groups; however, there is a significant difference in KT between smashers and spearers. Furthermore, if a smasher taxon and spearer taxon have the same Reach, the smasher is typically larger (based on carapace length) with a lower KT than the spearer. (D) A similar pattern is visible in the relationship between Reach and MA.**

association (Fig. 5B, D, Table 3). Figure 5 illustrates the associations between Reach, KT, and MA in two ways: using a "size-corrected" Reach, which has been divided by carapace length (Fig. 5A, B), and using the "raw" Reach measures (Fig. 5C, D). Our statistical analyses incorporated size as a variable and did not use this size correction; we use it here to simply visualize the relationships captured by the PGLS analyses.

When PGLS models are run comparing KT with just Reach or just size, as opposed to the above models in which size is incorporated into the comparisons between metrics, no significant association is found (Tables 3 and 4) indicating that neither is enough alone to explain variation in KT. The model that includes size as a factor also shows a higher likelihood than the models that compare size separately (KT~Reach vs. KT~Reach × Size: $\chi^2 = 22.463$, $P < 0.001$; KT~Size vs. KT~Reach × Size: $\chi^2 = 23.717$, $P < 0.001$). The same pattern holds true for comparisons of MA with Reach and size (MA~Reach vs. MA~Reach × Size: $\chi^2 = 35.479$, $P < 0.001$; MA~Size vs. MA~Reach × Size: $\chi^2 = 34.52$, $P < 0.001$).

Furthermore, all three metrics show a significant correlation (Table 4) with appendage type: KT and Reach are larger in spearers + *Hemisquilla*, whereas MA is larger in the smashers. When appendage type is included as a categorical factor in the PGLS test, the results are essentially the same as when KT, MA, and Reach are compared without it (Table 5). Removing *Hemisquilla* from the analysis did not alter the results.

Table 3. Analysis of biomechanical variables with and without incorporating size (carapace length) as a predictor variable using general linear models as implemented in PGLS.

y-Variable	*x*-Variable	Estimate	SE	*t*-Value	*P*-Value
KT (df = 2,34; λ = 0.842; LogLik = 18.057; R^2 = 0.04)	Intercept	**1.812**	**0.126**	**14.36**	**<0.001**
	Reach	0.0362	0.0303	1.195	0.241
KT (df = 4,33; λ = 0.551; LogLik = 29.29; R^2 = 0.549)	Intercept	**1.90**	**0.091**	**20.9**	**<0.001**
	Reach	**0.669**	**0.107**	**6.27**	**<0.001**
	Size	**−0.726**	**0.12**	**−5.925**	**<0.001**
MA (df = 2,34; λ = 1.0; LogLik = –5.14; R^2 = 0.001)	Intercept	**−3.351**	**0.247**	**−13.593**	**<0.001**
	Reach	0.0067	0.0506	0.132	0.895
MA (df = 4,33; λ = 0.98; LogLik = 12.604; R^2 = 0.631)	Intercept	**−3.421**	**0.153**	**−22.31**	**<0.001**
	Reach	**−1.33**	**0.18**	**−7.393**	**<0.001**
	Size	**1.488**	**0.198**	**7.504**	**<0.001**
KT (df = 2,34; λ = 0.658; LogLik = 40.87; R^2 = 0.748)	Intercept	**0.548**	**0.142**	**3.862**	**0.0005**
	MA	**−0.413**	**0.041**	**−10.035**	**<0.001**

Mean values for each species were log-transformed. Statistically significant values are indicated in bold. The statistical results apply to the coefficient.

Table 4. Appendage type (smasher vs. spearer + *Hemisquilla*) is correlated with KT, MA, and Reach.

y-Variable	Intercept	Coefficient	SE	*t*-Value	*P*-value	R^2	λ	Log-likelihood
KT (df = 2,34)	**1.7***	**0.285**	**0.092**	**3.11**	**<0.001**	**0.22**	**0.733**	**21.23**
MA (df = 2,34)	**−2.705***	**−0.74**	**0.206**	**−3.59**	**0.001**	**0.28**	**0.951**	**0.11**
Reach (df = 2,34)	**2.398***	**0.97**	**0.241**	**4.041**	**0.0003**	**0.32**	**0.000**	**−38.4**

Mean values for each species were analyzed using PGLS with all continuous variables log-transformed. Because the lone predictor for these PGLS analyses is a categorical variable (appendage type), they act as phylogenetically controlled *t*-tests (Organ et al. 2007). Statistically significant values are indicated in bold. The statistical results apply to the coefficient. An asterisk indicates that the intercept is significantly different than zero.

Table 5. Analysis of biomechanical variables incorporating appendage type as a predictor variable using general linear models as implemented in PGLS.

y-Variable	*x*-Variable	Estimate	SE	*t*-Value	*P*-Value
KT (df = 4,32; λ = 0.000; LogLik = 31.07; R^2 = 0.785)	Intercept	**1.88**	**0.076**	**24.835**	**<0.001**
	Reach	**0.627**	**0.112**	**5.604**	**<0.001**
	Type	0.11	0.059	1.875	0.07
	Size	**−0.705**	**0.123**	**−5.747**	**<0.001**
MA (df = 4,32; λ = 0.000; LogLik = 17.59; R^2 = 0.913)	Intercept	**−3.39**	**0.11**	**−30.897**	**<0.001**
	Reach	**−1.448**	**0.162**	**−8.935**	**<0.001**
	Type	**−0.34**	**0.085**	**−3.99**	**0.0004**
	Size	**1.676**	**0.18**	**9.322**	**<0.001**
KT (df = 3,33; λ = 0.681; LogLik = 41.08; R^2 = 0.748)	Intercept	0.509	0.156	3.271	0.0025
	MA	**−0.435**	**0.0532**	**−8.166**	**<0.001**
	Type	−0.041	0.065	−0.632	0.531

Mean values for each species were log-transformed. Size (carapace length) is included as a predictor when Reach is included in the model. Statistically significant values are indicated in bold. The statistical results apply to the coefficient.

HYPOTHESIS 2: ADAPTIVE MODELS

The results of the evolutionary model analyses support our second hypothesis. Specifically, the evolutionary model analysis shows that a multiple peak OU model is a better fit for the data than a simple Brownian motion or single-peak OU model. This finding was consistent for all metrics tested (Table 6). This evolutionary pattern can be seen graphically via a phylomorphospace of KT and Reach (Fig. 6). The multipeak OU model indicates that smashers evolve toward lower KT and lower Reach whereas spearers increase in Reach and KT (Fig. 6). Interestingly, the two

Table 6. Model comparisons for biomechanical metrics across stomatopod phylogeny.

	AICc	σ^2	α	θ
KT				
Brownian	−26.219	0.0564	NA	NA
OU single peak	−23.13	0.0789	0.749	1.928
OU multipeak	**−29.414**	0.103	2.027	1.598, 1.99
Reach				
Brownian	102.501	2.015	NA	NA
OU single peak	92.468	5.163	3.648	3.065
OU multipeak	**85.408**	12.607	12.833	2.459, 3.379
MA				
Brownian	14.653	0.176	NA	NA
OU single peak	20.85	0.195	0.16	−3.334
OU multipeak	**12.37**	0.163	0.376	−0.321, −3.467

Bold values indicate the best-supported metric. AICc = Akaike information criterion corrected for finite sample sizes (Burnham and Anderson 2002); σ^2 = Brownian motion rate parameter; θ = strength of selection; θ = optimal trait value (there are two for the multipeak model).

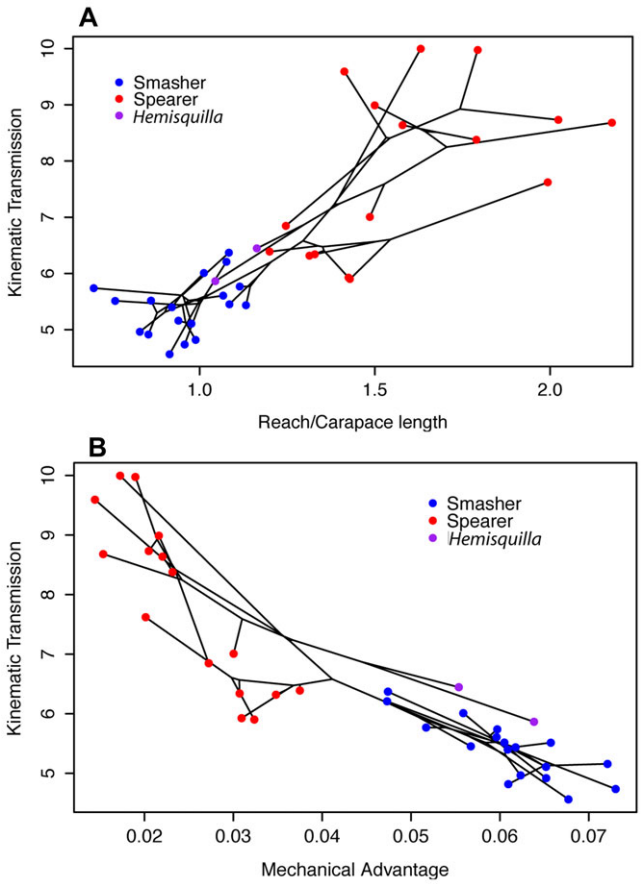

Figure 6. Two phylomorphospaces illustrate the disparate evolutionary variation of our biomechanical metrics overlaid with the stomatopod tree topology. (A) Phylomorphospace of Reach/size versus KT. (B) Phylomorphospace of MA versus KT. Smashers (in blue) represent a monophyletic clade within the stomatopods that trends toward low values of both KT and Reach/size and high values of MA. This combination implies low appendage extension combined with strikes with potentially high force and speed. Spearers (in red) exhibit a wider range of evolutionary variation in KT and Reach/size, yet their lowest values of KT and Reach/size nearly always exceed the highest values in smashers. Spearers also show low values of MA. The two *Hemisquilla* species (in purple) fall at the intersection of smasher and spearers in terms of KT and Reach/size, yet fall within the smasher range for MA. Note that the taxa with the highest values of Reach/size and KT and lowest values of MA are not necessarily all closely related, potentially illustrating multiple invasions of this morphospace by spearing clades.

Hemisquilla taxa at the base of the tree show intermediate values for both KT and Reach. When the two *Hemisquilla* taxa are removed, the results change very little and the multipeak model remains the best-supported model (Table 7). The phylogenetic Monte Carlo simulations also show that the multipeak OU model is better supported than the single-peak model (see Fig. S1). The distributions of the likelihood statistic for KT, MA, and Reach also show relatively low overlap between models, indicating that we have the power to distinguish between them and that the observed likelihood ratio (dashed line) falls well within the multipeak distribution (see Fig. S1). Ancestral state reconstructions of appendage type are mapped onto phylogeny in Figure 4.

Discussion

The evolutionary diversification of mantis shrimp appendages supports the hypothesis that the linkage and lever systems exhibit correlated evolutionary change and that these changes occur synergistically. Specifically, we found synergistic force amplification in smashers and displacement amplification in spearers + *Hemisquilla*. KT, MA, and Reach are correlated across stomatopod phylogeny, such that both the linkage and lever systems show tandem amplification of force and displacement. Further, KT, MA, and Reach follow distinct evolutionary patterns across stomatopod phylogeny. Spearers + *Hemisquilla* exhibit displacement amplification (high KT, low MA, and high Reach) whereas smashers show force amplification (low KT, high MA). All of our results remain consistent when *Hemisquilla* is removed from the analyses, so throughout the discussion we will refer to "spearers + *Hemisquilla*" as simply "spearers." This synergistic relationship between the linkage and lever mechanisms in stomatopod appendages appears to be largely independent of appendage type.

Table 7. Model comparisons for biomechanical metrics as in Table 6, but with the two *Hemisquilla* taxa removed from the analysis.

	AICc	σ^2	α	θ
KT				
Brownian	−25.447	0.0517	NA	NA
OU single peak	−21.476	0.0686	0.572	1.966
OU multi peak	**−28.989**	0.0927	1.938	1.609, 2.034
Reach				
Brownian	96.486	1.866	NA	NA
OU single peak	87.818	4.856	3.438	2.989
OU multi peak	**82.351**	11.404	11.239	2.46, 3.326
MA				
Brownian	9.925	0.146	NA	NA
OU single peak	16.243	0.163	0.158	−3.553
OU multi peak	**−0.735**	0.196	1.72	−2.551, −3.728

Bold values indicate the best-supported metric. AICc = Akaike information criterion corrected for finite sample sizes (Burnham and Anderson 2002); σ^2 = Brownian motion rate parameter; α = strength of selection; θ = optimal trait value (there are two for the multipeak model).

Our results show that coupled, yet independent, mechanical systems can act consistently during evolutionary diversification.

KT, REACH, AND SIZE

High KT in the stomatopod linkage system is tightly associated with displacement. Appendages with high KT maximize their extension (low MA and high Reach) during prey capture at the expense of force; appendages with low KT have high MA and low Reach. High KT in an aquatic setting can also induce high levels of drag that reduce appendage speed (McHenry et al. 2012). Smashers gain both force and speed by giving up high displacement. The overall high KT in stomatopods (relative to linkages in teleost fish) is likely required to overcome a limited range of input motion (10°–15° rotation of the meral-V; Patek et al. 2007). High KT allows these minimal input rotations to be translated into much greater output rotations.

Neither KT nor MA shows significant associations with body size (carapace length). However, when the associations of KT with Reach and size are separated from each other (Table 3), KT does show a negative relationship with size. We would expect KT and body size to be negatively correlated based on the implication from previous work that both higher KT and larger size will increase the drag (McHenry et al. 2012). This prediction is based on the assumption that reducing drag is of paramount importance to the evolution of the stomatopod strike system, and that selection would favor either larger animals with low KT or smaller ones with larger KT.

Smashers and spearers have a similar range of Reach, while still showing a strong separation in KT (Fig. 5C). Specifically, spearers have higher KT than smashers with the same value of Reach. However, if smashers and spearers with similar Reach are compared, then smasher body size tends be larger than spearer body size. (Fig. 5C). The correlation between Reach and KT holds even when appendage types are included as confounding factors. The relationship between these metrics and appendage type is explored to a great extent in the next section.

SMASHERS VERSUS SPEARERS (AND *HEMISQUILLA*)

The evolution of the raptorial appendage is best modeled as a multipeak OU model, in which smashers and spearers evolve toward distinct optima. Smashers show an evolutionary trend toward reduced KT and Reach, leading to less displacement or extension of the appendage. On the other hand, spearers consistently increase KT and Reach, resulting in appendages with large extensions that move more slowly than those of smashers. Convergent evolution may have occurred in the most extreme values for KT and Reach. These extremes in KT and Reach are found in spearers that are not all closely related (Fig. 6). Although grouped with the spearers based on phylogenetic placement, *Hemisquilla* spp. do not fit into either the smasher or spearer category. They are scavengers/foragers that dislodge and crush hard-shelled prey without the bulbous hammer-shaped appendages of smashers (Basch and Engle 1989, 1993). They have intermediate values of KT and Reach (Fig. 5), with MA well within the range of smashers (Fig. 5). Removing them from the analysis made little difference although the multipeak model becomes slightly better supported (compare Tables 6 and 7).

Drawing a definitive connection between mechanics and kinematics is challenging in this system. Presumably, spearers need to be somewhat fast to successfully ambush prey. However, the speed required for evasive prey capture might be less than that required to achieve sufficient momentum to smash hard-shelled prey. This is supported by recent work illustrating that spearers strike an order of magnitude more slowly than smashers (deVries et al. 2012). The slower speed in spearers may be due to a trade-off with displacement: an appendage built for greater displacement will accrue greater drag due to the size of the appendage and high KT. Further evidence for a potential hydrodynamic limit can be seen in Figure 5A. Although the main trend shows a tight positive correlation between Reach and KT, a different pattern can be seen when KT values exceed ~7.0 (2 on the log scale in Fig. 5A). Above that value, there appears to be a negative correlation between KT and Reach. The amount of extension/displacement may

be constrained, such that stomatopods with the longest Reach have slightly lower KT.

The results of the present study offer insights into recent modularity analyses of the raptorial appendage. Modularity can be analyzed at various levels of biological organization, including developmental, functional, and evolutionary (Klingenberg et al. 2010; Claverie et al. 2011, Claverie and Patek 2013). Even though the raptorial appendage shows developmental and evolutionary modularity of the shapes of the raptorial appendage components (Claverie et al. 2011, Claverie and Patek 2013), we found tight integration at the functional, mechanical level. In other words, even though appendage components can vary independently at developmental and evolutionary levels, the biomechanical outputs remain tightly coordinated along a force/displacement continuum.

The correlated evolution of the mechanical components of the raptorial appendage, along with the modularity of their shapes at developmental and evolutionary levels, corroborates recent findings dissociating developmental and functional modules (Klingenberg et al. 2010). Developmental integration is often thought to be associated with developmental constraints, preventing the independent evolution of related morphological units. However, developmental, evolutionary, and functional modules need not always match (Breuker et al. 2006; Klingenberg et al. 2010). Indeed, it is possible that in mantis shrimp, even if an intrinsic genetic structure allows the appendages to develop in three independent units (Claverie et al. 2011), and evolutionary processes drive the evolution of two modular units at variable rates (Claverie and Patek 2013), selective pressures acting on function may have constrained the functional components to coevolve. Thus, variation in the components of power-amplified systems is likely controlled by different processes at the developmental, evolutionary, and functional levels.

MANY-TO-ONE MAPPING

Many-to-one mapping posits that mechanical systems with more than one degree of freedom will show mechanical redundancy and promote diversification by allowing for morphological evolution without compromising functionality (Alfaro et al. 2004, 2005; Wainwright et al. 2005). Although our study examined the interplay between multiple mechanisms, many-to-one mapping is generally identified at the level of a single mechanism, such that the function can be expressed as a single variable (KT, suction index, etc.). Given that the linkage and lever systems each independently produces force or displacement amplification, it should be possible for the linkage and lever systems to evolve independently and produce a pattern similar to many-to-one mapping. Reduction in force amplification of the linkage (high KT) could be counterbalanced by an increase in force amplification through the lever (high MA), maintaining a stable overall output of force amplification. This should allow for greater diversity in the underlying mechanisms while maintaining a consistent overall output, analogous to many-to-one mapping.

However, our examination of the coordination of two coupled, but independent, mechanisms does not show a pattern of independent evolution. The functional outputs of the lever and linkage are tightly, negatively correlated such that the result is always a tandem amplification of either force or displacement (Fig. 5). These tight negative correlations result in a large, empty area of the phylomorphospace (Fig. 6). Perhaps stomatopods that we have yet to study would fill this space; however, *Hemisquilla* represents a distinct appendage morphology that still falls within the general pattern. Perhaps the hydrodynamic pressures discussed above are too strong to allow stomatopods to explore those empty regions of morphospace. Regardless of the reason, multiple mechanisms working in concert do not exhibit an equivalent pattern to many-to-one mapping, but instead a more restricted evolutionary pattern. Further research is needed to verify and explore these ideas.

CONCLUSIONS

The stomatopod raptorial appendage consists of a linkage and a lever working in tandem to drive an extremely rapid strike. The biomechanical outputs of each mechanism show correlated and congruent evolution. Stomatopods exhibit divergent evolution such that consistent amplification of either force or displacement occurs within groups defined by appendage type. Specifically, spearers produce slower, weaker strikes with a large spatial range and smashers exhibit high-force, high-speed strikes over a small range. The connection between morphological form and mechanical function is clear-cut and consistent both at proximate and evolutionary levels. Our results demonstrate that the mechanical redundancy that can occur within a single mechanism, such as fish four-bar linkages, does not necessarily scale to mechanical redundancy in coupled mechanisms. Thus, the dynamics of biomechanical evolution can operate differently when considered at the single-mechanism level as compared to the level of multiple, coupled mechanisms. Future research on the multilevel dynamics of biomechanical evolution stands to illuminate the complex interplay between physical rules and evolutionary diversification.

ACKNOWLEDGMENTS

The authors would like to thank S. Price for extensive assistance on phylogenetic comparative methods and L. Revell for help and advice for using his Phytools package for R. We would also like to thank M. Porter, M. Rosario, P. Green, S. Cox, and K. Kagaya for helpful discussions on stomatopod biology as well as two anonymous reviewers for their insightful comments, which have greatly improved the quality of this

article. We also thank K. Reed (National Museum of Natural History, Washington, DC) and S. Keable (Australian Museum of Natural History, Sydney) for access to their specimen collections. This work was funded by the National Science Foundation (IOS-1149748) to SNP. The authors declare no conflict of interest.

DATA ARCHIVING

The doi for our data is 10.5061/dryad.m8q8h.

LITERATURE CITED

Ahyong, S. T., and S. N. Jarman. 2009. Stomatopod interrelationships: preliminary results based on analysis of three molecular loci. Arth. Syst. Phylo. 67:91–98.

Alfaro, M. E., D. I. Bolnick, and P. C. Wainwright. 2004. Evolutionary dynamics of complex biomechanical systems: an example using the four-bar mechanism. Evolution 58:495–503.

Alfaro, M. E., D. I. Bolnick, and P. C. Wainwright. 2005. Evolutionary consequences of many-to-one mapping of jaw morphology to mechanics in labrid fishes. Amer. Nat. 165:E140–E154.

Anderson, P. S. L., and M. W. Westneat. 2009. A biomechanical model of feeding kinematics for *Dunkleosteus terrelli* (Arthrodira, Placodermi). Paleobiology 35:251–269.

Anderson, P. S. L., M. Friedman, M. D. Brazeau, and E. J. Rayfield. 2011. Initial radiation of jaws demonstrated stability despite faunal and environmental change. Nature 476:206–209.

Anker, G. Ch. 1974. Morphology and kinetics of the stickleback, *Gasterosteus aculeatus*. Trans. Zool. Soc. 32:311–416.

Barel, C. D. N., J. W. van der Meulen, and H. Berkhoudt. 1977. Kinematischer Transmissionskoeffizient und Vierstangensystem als Funktionsparameter und Formmodell fur mandibulare Depressionsapparate bei Teleostiern. Anat. Anz. 142:21–31.

Basch, L. V., and J. M. Engle. 1989. Aspects of the ecology and behavior of the stomatopod *Hemisquilla ensigera californiensis* (Gonodactyloidea: Hemisquillidae). Pp. 199–212 *in* E. A. Ferrero, ed. Biology of stomatopods. Vol. 3. Mucchi, Modena.

———. 1993. Biogeography of *Hemisquilla ensigera californiensis* (Crustacea: Stomatopoda) with emphasis on Southern California bight populations. Pp. 211–220 *in* F. G. Hochberg, ed. Third California Islands symposium. Santa Barbara Museum of Natural History, Santa Barbara, CA.

Boettiger, C., G. Coop, and P. Ralph. 2012. Is your phylogeny informative? Measuring the power of comparative methods. Evolution 66:2240–2251.

Breuker, C. J., V. Debat, and C. P. Klingenberg. 2006. Functional evo-devo. Trends Ecol. Evol. 21:488–492.

Burnham, K. P., and D. R. Anderson. 2002. Model selection and multimodel inference: a practical information theoretic approach. Springer, New York.

Butler, M. A., and A. A. King. 2004. Phylogenetic comparative analysis: a modeling approach for adaptive evolution. Am. Nat. 164: 683–695.

Caldwell, R. L., and H. Dingle. 1976. Stomatopods. Sci. Amer. 234: 80–89.

Claverie, T., and S. N. Patek. 2013. Modularity and rates of evolutionary change in a power-amplified prey capture system. Evolution 67:3191–3207.

Claverie, T., E. Chan, and S. N. Patek. 2011. Modularity and scaling in fast movements: power amplification in mantis shrimp. Evolution 65:443–461.

Collar, D. C., and P. C. Wainwright. 2006. Discordance between morphological and mechanical diversity in the feeding mechanism of centrarchid fishes. Evolution 60:2575–2584.

Cox, S. M., D. Schmidt, Y. Modarres-Sadeghi, and S. N. Patek. 2014. A physical model of the extreme mantis shrimp strike: kinematics and cavitation of Ninjabot. Bioinspir. Biomim. 9:1–16.

deVries, M., E. A. K. Murphy, and S. N. Patek. 2012. Strike mechanics of an ambush predator: the spearing mantis shrimp. J. Exp. Biol. 215:4374–4384.

Dingle, H., and R. L. Caldwell. 1978. Ecology and morphology of feeding and agonistic behavior in mudflat stomatopods (Squillidae). Biol. Bull. 155:134–149.

Ho, S. Y. W., and M. J. Phillips. 2009. Accounting for calibration uncertainty in phylogenetic estimation of evolutionary divergence times. Sys. Biol. 58:367–380.

King, A. A., and M. A. Butler. 2009. OUCH: Ornstein-Uhlenbeck models for phylogenetic comparative hypotheses (R package). Available at http://ouch.r-forge.r-project.org.

Klingenberg, C. P., V. Debat, and D. A. Roff. 2010. Quantitative genetics of shape in cricket wings: developmental integration in a functional structure. Evolution 64:2935–2951.

McHenry, M. J., T. Claverie, M. V. Rosario, and S. N. Patek. 2012. Gearing for speed slows the predatory strike of a mantis shrimp. J. Exp. Biol. 215:1231–1245.

Organ C. L., A. M. Shedlock, A. Meade, M. Pagel, and S. V. Edwards. 2007. Origin of avian genome size and structure in nonavian dinosaurs. Nature 446:180–184.

Orme, D., R. Freckleton, G. Thomas, T. Petzoldt, S. Fritz, N. Isaac, and W. Pearse. 2012. caper: comparative analyses of phylogenetics and evolution in R. R package version 0.5.

Paradis, E., J. Claude, and K. Strimmer. 2004. APE: analyses of phylogenetics and evolution in R language. Bioinformatics 20:289–290.

Patek, S. N., and R. L. Caldwell. 2005. Extreme impact and cavitation forces of a biological hammer: strike forces of the peacock mantis shrimp *Odontodactylus scyllarus*. J. Exp. Biol. 208:3655–3664.

Patek, S. N., W. L. Korff, and R. L. Caldwell. 2004. Deadly strike mechanism of a mantis shrimp. Nature 428:819–820.

Patek, S. N., B. N. Nowroozi, J. E. Baio, R. L. Caldwell, and A. P. Summers. 2007. Linkage mechanics and power amplification of the mantis shrimp's strike. J. Exp. Biol. 210:3677–3688.

Porter, M. L., Y. Zhang, S. Desai, R. L. Caldwell, and T. W. Cronin. 2010. Evolution of anatomical and physiological specialization in the compound eyes of stomatopod crustaceans. J. Exp. Biol. 213:3473–3486.

R Development Core Team. 2012. R: a language and environment for statistical computing. R Foundation for Statistical Computing, Vienna, Austria.

Rayner, J. 1988. Form and function in avian flight. Curr. Ornith. 5: 1–66.

Revell, L. J. 2012. phytools: an R package for phylogenetic comparative biology (and other things). Methods Ecol. Evol. 3:217–223.

Suh, C. H., and C. W. Radcliffe. 1978. Kinematics and mechanisms design. Wiley and Sons, New York.

Uicker, J. J., G. R. Pennock, and J. E. Shigley. 2003. Theory of machines and mechanisms. Oxford Univ. Press, New York.

Wainwright, P. C., M. E. Alfaro, D. I. Bolnick, and C. D. Hulsey. 2005. Many-to-one mapping of form to function: a general principle in organismal design? Integr. Comp. Biol. 45:256–262.

Warner, G. F., and A. R. Jones. 1976. Leverage and muscle type in crab chelae (Crustacea: Brachyura). J. Zool. 180:57–68.

Westneat, M. W. 1994. Transmission of force and velocity in the feeding mechanisms of labrid fishes (Teleostei, Perciformes). Zoomorph 114:103–118.

Yang, Z., N. Goldman, and A. Friday. 1995. Maximum likelihood trees from DNA sequences: a peculiar statistical problem. Syst. Biol. 44:384–399.

Associate Editor: D. Carrier

Supporting Information

Additional Supporting Information may be found in the online version of this article at the publisher's website:

Figure S1. Phylogenetic Monte Carlo (PMC) results for all traits comparing single-peak (null, orange) and multipeak (test, green) OU models.